

Super lithium-rich K giant with low ^{12}C to ^{13}C ratio \star

Y.T. Zhou^{1,2}, J.R. Shi^{1,2}, H.L. Yan¹, Q. Gao¹, J.B. Zhang^{1,2}, G. Zhao^{1,2}, K. Pan^{1,3}, and Y. B. Kumar¹

¹ Key Laboratory of Optical Astronomy, National Astronomical Observatories, Chinese Academy of Sciences, Beijing 100012, China.

e-mail: sjr@nao.cas.cn

² University of Chinese Academy of Sciences, Beijing 100049, China.

³ Apache Point Observatory and New Mexico State University, P.O. Box 59, Sunspot, NM, 88349-0059, USA.

Received 03 January 2017/ Accepted 8 March 2018

ABSTRACT

Context. The lithium abundances in a few percent of giants exceed the value predicted by the standard stellar evolution models, and the mechanisms of Li enhancement are still under debate. The Large Sky Area Multi-Object Fiber Spectroscopic Telescope (LAMOST) survey has obtained over six million spectra in the past five years, and thus provides a great opportunity to search these rare objects and to more clearly understand the mechanisms of Li enhancement.

Aims. The aim of this work is to accurately measure the Li abundance and investigate the possible mechanisms of Li enrichment for a newly found super Li-rich giant, TYC 3251-581-1, located near the luminosity function bump with a low carbon isotopic ratio.

Methods. Based on the high-resolution spectrum we obtained the stellar parameters (T_{eff} , $\log g$, $[\text{Fe}/\text{H}]$), and determined the elemental abundances of Li, C, N, α , Fe-peak, r-process, s-process elements, and the projected rotational velocity. For a better understanding of the effect of mixing processes, we also derived the ^{12}C to ^{13}C ratio, and constrained the evolutionary status of TYC 3251-581-1 based on the BaSTI stellar isochrones.

Results. The super Li-rich giant TYC 3251-581-1 has $A(\text{Li}) = 3.51$, the average abundance of two lithium lines at $\lambda = 6708 \text{ \AA}$ and 6104 \AA based on the non-local thermodynamic equilibrium (NLTE) analysis. The atmospheric parameters show that our target locates on the luminosity function bump. The low carbon isotopic ratio ($^{12}\text{C}/^{13}\text{C} = 9.0$), a slow rotational velocity $v \sin i = 2.2 \text{ km s}^{-1}$, and no sign of IR excess suggest that additional mixing after first dredge up (FDU) should occur to bring internal synthesized Li to the surface. The low carbon ($[\text{C}/\text{Fe}] \sim -0.34$) and enhanced nitrogen ($[\text{N}/\text{Fe}] \sim 0.33$) are also consistent with the sign of mixing.

Conclusions. Given the evolutionary stage of TYC 3251-581-1 with the relatively low $^{12}\text{C}/^{13}\text{C}$, the internal production which replenishes Li in the outer layer is the most likely origin of Li enhancement for this star.

Key words. Stars: abundances - stars: chemically peculiar - stars: individual (TYC 3251-581-1) - stars: late-type

1. Introduction

It is predicted that lithium is destroyed considerably throughout the lifetime for the giants, the dilution of lithium occurs when the convective envelope circulates the surface materials to the deep regions where the temperature is high enough (about several million Kelvin) to destroy Li. According to the standard stellar models, the significant depletion of surface Li takes place during the first dredge-up (FDU) in low mass stars (e.g. Iben 1967b,a). The standard models predicted that the Li abundance of low-mass stars with solar metallicity is less than about 1.5 dex when the star evolves to the end of the FDU on the red giant branch (RGB, Charbonnel & Lagarde 2010), and it is suggested that the Li abundance would be further declined after the RGB bump because of the burning by the extra mixing (e.g. Charbonnel & Zahn 2007; Charbonnel & Lagarde 2010). However, numerous observations show that a few percent of giants hold an Li abundance higher than 1.5 dex (e.g. Brown et al. 1989; de la Reza et al. 1997; Kumar et al. 2011; Adamów et al. 2014). These so-called Li-rich stars provide a challenge to the standard stellar evolution models.

After the discovery of the first Li-rich K giant star (Wallerstein & Sneden 1982), various scenarios, including the effects of external sources and internal production, have been envisaged to interpret such ‘anomalous’ abundance. Suggested external sources include contamination by the ejecta of nearby novae (Martin et al. 1994), mass transfer from the Li-enhanced companion (Kirby et al. 2016), and the engulfment of planets and/or brown dwarfs (Alexander 1967; Siess & Livio 1999). On the other hand, Sackmann & Boothroyd (1999) proposed that Li is freshly synthesized inside stars known as cool bottom processing, in this process, ^3He enriched after the FDU can be burned into ^7Be at the regions that have high enough temperature, ^7Be is then transported to a cooler zone, where it captures an electron and decays into ^7Li (Cameron & Fowler 1971, hereafter, CF mechanism).

Several studies have been devoted to investigating the issue of reconciling the existence of Li-rich giants. Charbonnel & Balachandran (2000) proposed that Li-rich giants could be formed at the specific evolutionary stages, that is, the RGB bump for low mass stars, and the early asymptotic giant branch (AGB) for intermediate-mass stars. In such cases, when the hydrogen burning shell in the stars erases the discontinuity in the mean molecular weight left behind at the end of FDU, the extra-mixing is expected to trigger the CF mechanism to produce fresh Li. Nevertheless, Kumar et al. (2011) found the Li-rich giants clustered

\star Based on observations obtained with the Apache Point Observatory 3.5-metre telescope, which is owned and operated by the Astrophysical Research Consortium.

around the red clump and the horizontal branch, then they suggested that the onset of CF mechanism might locate at these evolutionary stages. However, other observational results indicate that Li-rich stars can be found almost anywhere along the RGB (Monaco et al. 2011; Lebzelter et al. 2012; Martell & Shetrone 2013). Among ~ 170 of the Li-rich giants included the Li-rich collection of Casey et al. (2016) with seven new-found by Li et al. (2018), only ~ 20 super Li-rich giants (Adamów et al. 2015) with Li abundance higher than 3.3 dex¹ have been found up to now (e.g. Kumar & Reddy 2009; Martell & Shetrone 2013; Monaco et al. 2014; Casey et al. 2016).

In the past five years LAMOST has obtained spectra for six million stars, and the number is still increasing (Cui et al. 2012; Zhao et al. 2012). It is an ideal database in which to seek Li-rich giant candidates because of the huge number of spectra (Silva Aguirre et al. 2014; Li et al. 2016). In this paper, we report a new discovery of super Li-rich giant from the LAMOST survey, TYC 3251-581-1, and its follow-up observations with the 3.5 m telescope at the Apache Point Observatory (APO). The paper is organized as follows. In Sect. 2 we briefly describe the observation and data reduction, and in Sect. 3 we present the details of the determinations of the stellar parameters and elemental abundances. Finally, we discuss the potential scenarios of Li enhancement based on the evolutionary status of this star in Sect. 4.

2. Observations

This candidate Li-rich giant was found with the LAMOST low resolution spectrum, and selected based on the visual inspection of the spectrum and the measurement of equivalent width for the Li resonance line. The high-resolution and high S/N spectra for TYC 3251-581-1 were obtained by the cross-dispersed échelle spectrograph mounted on the 3.5 m telescope at the APO. The wavelength coverage is from 3200 to 10000 Å with a resolution of $\sim 31,500$. The star was observed three times with a total integration time of 1.5 hours on Oct. 22, 2014. The S/N is ~ 160 at 6708 Å.

The observed data were reduced with the revised automatic IDL programme, which was designed for the FOCES échelle spectrograph (Pfeiffer et al. 1998). The standard procedures were applied to extract one-dimensional spectra, and the uncertainty in wavelength calibration is less than 0.01 Å.

3. Spectroscopic analysis

3.1. Atmospheric parameters

The stellar parameters were determined with a standard procedure based on the MAFAGS-OS atmospheric model (Grupp et al. 2009). The effective temperature (4670 ± 80 K) was estimated by requesting the same abundance from the neutral iron lines with different excitation potentials, which is in good agreement with the photometric temperature of 4650 K (V-K) obtained by the calibrations of Alonso et al. (1999). The spectroscopic surface gravity is derived by minimizing the difference between the abundances measured from Fe I and Fe II lines. The result is consistent with the trigonometric gravity ($\log g_{\text{Gaia}}$), which is based on the parallax of $\sim 0.58 \pm 0.30$ mas reported by the recently released Gaia DR1 (Gaia Collaboration et al. 2016). The trigonometric gravity is calculated through

$$\log g = \log g_{\odot} + \log\left(\frac{M}{M_{\odot}}\right) + 4 * \log\left(\frac{T_{\text{eff}}}{T_{\text{eff}\odot}}\right) + 0.4 * (M_{\text{bol}} - M_{\text{bol}\odot}), \quad (1)$$

¹ the Li abundance in meteorite (Asplund et al. 2009)

Table 1. Stellar parameters, kinematics information for TYC 3251-581-1

Property	Value	Reference
Position (J2000)	R.A. 00:20:36.35 DEC. +46:59:05.05	
Magnitudes	B 11.94 V 11.04 K ₂ MASS 8.256	Høg et al. (2000) Høg et al. (2000) Cutri & et al. (2013)
π [mas]	0.58 ± 0.30	Gaia Collaboration et al. (2016)
V_{helio}	-34.68 ± 0.06	This work
U_{LSR} [km s ⁻¹]	34.3	This work
V_{LSR}	-23.51	This work
W_{LSR}	-15.82	This work
[Fe/H]	-0.09 ± 0.10	This work
T_{eff} [K]	4670 ± 80	This work
$\log g$ [cm s ⁻²]	2.30 ± 0.20	This work
$\log g_{\text{Gaia}}$ [cm s ⁻²]	2.28 ± 0.50	This work
ξ_t [km s ⁻¹]	1.57 ± 0.20	This work
$v \sin i$ [km s ⁻¹]	2.2 ± 0.3	This work
Mass [M_{\odot}]	2.16 ± 1.85	This work
Age [Gyr]	0.72 ± 5.30	This work
Log (L/L_{\odot})	2.12 ± 0.50	This work
Radius [R_{\odot}]	17.27 ± 8.40	This work

where the absolute bolometric magnitude is estimated by the formula $M_{\text{bol}} = V_{\text{mag}} + 5 * \log \pi + 5.0 - A_V + BC$, the interstellar extinction is denoted as A_V , and the bolometric correction is derived by the empirical relations of Alonso et al. (1999). The microturbulent velocity was determined by requiring the abundance from Fe I lines being independent of their reduced equivalent widths. The derived stellar parameters are given in Table 1, along with the estimated errors in the stellar parameters. About 50 well separated and mild (20 \sim 100 mÅ) Fe I lines and eight Fe II lines were used in the parameter determination.

Stellar mass and age were derived based on the Gaia parallax, spectroscopic T_{eff} combined with the BaSTI Ver.5.0.1 evolutionary tracks (Pietrinferni et al. 2004). We employed the absolute bolometric magnitude M_{bol} and T_{eff} to match the theoretical calculations in the evolutionary tracks, which is based on the scaled solar metal mixture. In the process, the canonical model without overshooting was adopted. Following Pietrinferni et al. (2004), the theoretical tracks with exact metallicity $Z = 0.014$ were computed by interpolating on a point-by-point basis among the available grid of metallicities. The uncertainties were estimated by taking into account the errors of M_{bol} and T_{eff} . The stellar radius was derived by $R = \sqrt{GM_{\star}/g}$.

Following Adibekyan et al. (2012), we calculated the spatial velocity components, ($U_{\text{LSR}}, V_{\text{LSR}}, W_{\text{LSR}}$) = (34, -23, -16) km s⁻¹, and the distance away from the galactic plane $Z = 0.43$ kpc. According to the criteria of Reddy et al. (2006), TYC 3251-581-1 likely belongs to the thin disc with a probability of 98%.

3.2. Determinations of abundances

The Li abundance analysis was performed using the spectral synthesis method with the SIU software package developed by Reetz (1991) for the Li resonance line at $\lambda = 6708$ Å and the subordinate line at 6104 Å. The contributions from the other lines nearby have been considered, and the lithium abundance was obtained until the best fit was reached between the synthetic and observed spectra. For the resonance line, a local thermodynamic equilibrium (LTE) Li abundance is 3.68 dex by employing the line list compiled by Carlberg et al. (2012). Though the subordinate line at 6104 Å is usually very weak for the normal giants,

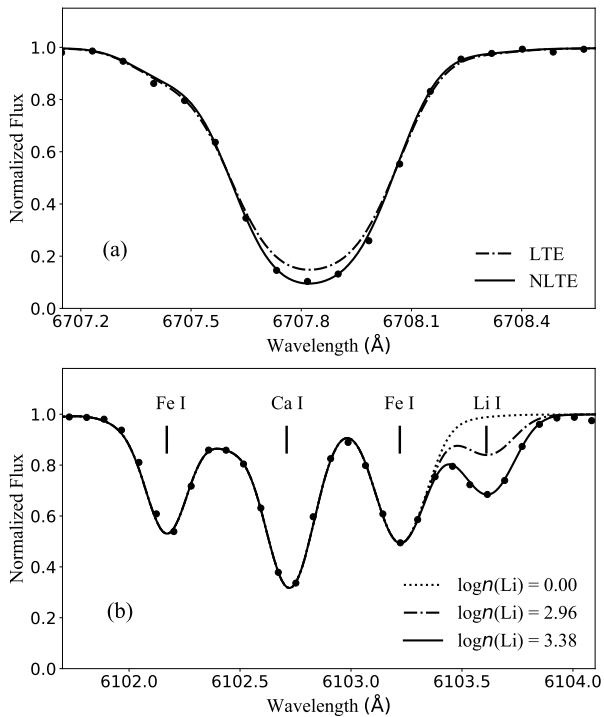


Fig. 1. Spectral synthesis of Li I line at 6708 Å (panel a), and the subordinate line at 6104 Å (panel b) for TYC 3251-581-1.

it is strong in our target, an LTE abundance of $A(\text{Li}) = 3.38$ dex (where $A(\text{Li}) = \log[n(\text{Li})/n(\text{H})] + 12$) is derived by adopting a line list from VALD database (Kupka et al. 1999). The uncertainties in the derived lithium abundances that arose because of the errors of the atmospheric parameters were evaluated to be 0.26 dex and 0.13 dex for Li lines at $\lambda = 6708$ Å and $\lambda = 6104$ Å (Table 2). We note that the synthetic spectrum at 6708 Å cannot reach the core of this line, as shown by the dashed line in Fig. 1. The high lithium giants suffer a large non-local thermodynamic equilibrium (NLTE) effect (Lind et al. 2009), we investigated the NLTE effects for the two lines based on the Li atomic model of Shi et al. (2007). When the NLTE effects included, our results show that the NLTE corrections² from the two lines at $\lambda = 6708$ Å and $\lambda = 6104$ Å are -0.20, +0.15 dex, respectively. The NLTE lithium abundances of 3.48 and 3.53 are obtained, leading to a smaller difference between two lines compared with those from the LTE analysis. The average of the NLTE abundances from the two lines was adopted as the final Li abundance with $A(\text{Li}) = 3.51$ dex. We also interpolated the NLTE corrections by using the grid of Lind et al. (2009), the corrections for the two lines at $\lambda = 6708$ Å and $\lambda = 6104$ Å are -0.22 and +0.18 dex, respectively. Their results are in good agreement with ours. In the process of NLTE analysis, we measured the uncertainties of NLTE correction due to errors of atmospheric parameters based on the method of Shi et al. (2007) (see Table 3). The differential NLTE correction is slightly larger of the resonance line than that of the subordinate line caused by the changes of stellar parameters, and the errors in T_{eff} and $\log g$ have a major effect on the uncertainties of NLTE correction.

The carbon abundances were derived from the synthesis of the C I line at 5380 Å, and the C₂ Swan bandheads at 5135 Å (Alexeeva & Mashonkina 2015). Since the neutral nitrogen lines

² The NLTE correction is denoted as: $\Delta_{\text{NLTE}} = \log n(\text{Li})_{\text{NLTE}} - \log n(\text{Li})_{\text{LTE}}$

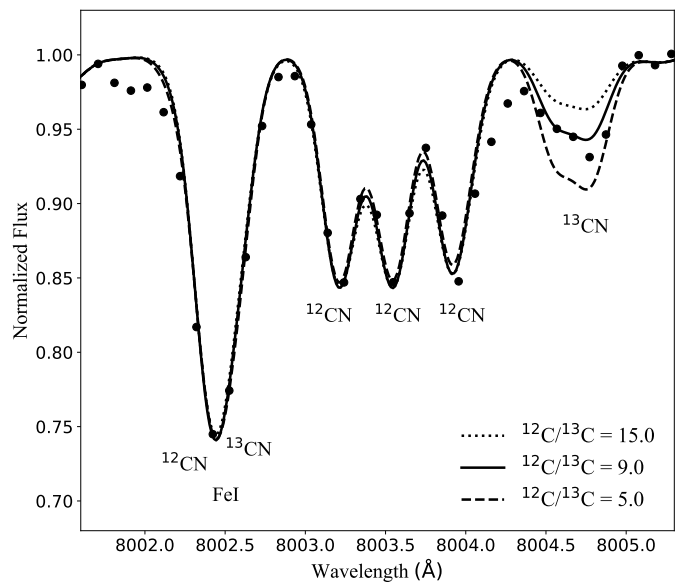


Fig. 2. Determination of the carbon isotopic ratio ^{12}C to ^{13}C for TYC 3251-581-1. The three synthetic spectra show ratios of 15 (dotted), 9 (solid, best fit) and 5 (dashed), respectively.

are either too weak or blended by the telluric absorption lines, we fixed the carbon abundance and determined the nitrogen abundance based on the CN bands near 8003 Å. The $[\text{C}/\text{Fe}] = -0.34$ and $[\text{N}/\text{Fe}] = 0.33$ show that our target is deficient in carbon, and enhanced in nitrogen (Table 2).

The interpretation of the source being Li-rich is likely to be associated with the extra mixing. The mixing process carries the internal material, which has undergone the CNO cycle to the surface, leading to a decrease in ^{12}C and increase in ^{13}C . It is suggested that the carbon isotopic ratio (^{12}C to ^{13}C) is a good indicator for tracing the stellar mixing process (Eggleton et al. 2008; Charbonnel & Lagarde 2010). We obtained the $^{12}\text{C}/^{13}\text{C}$ value by spectral synthesis for a small group of molecular lines from the region near 8003 Å, as shown in Fig. 2. The line list used for spectral synthesis is from Carlberg et al. (2012) and the derived $^{12}\text{C}/^{13}\text{C}$ is ~ 9.0 , which is much lower than that of the typical $^{12}\text{C}/^{13}\text{C}$ (~ 25) after the FDU (e.g. Eggleton et al. 2008; Palmerini et al. 2011).

For purpose of comparison (see Sec. 4), we also measured the abundances of the odd-Z (Na, Al), α (Mg, Si, Ca, and Ti), Fe-peak (Sc, V, Cr, Mn, Co, Ni, and Zn), and neutron capture elements (Y, Ba, La, Nd, Eu) with the spectral synthesis method, and the detailed chemical abundances are reported in Table 2. The derived abundances of α elements ($[\text{Mg}/\text{Fe}]$, $[\text{Si}/\text{Fe}]$, and $[\text{Ti}/\text{Fe}]$) are 0.06 dex, 0.03 dex, and -0.09 dex, respectively, which are in agreement with that of the typical thin disc star (Adibekyan et al. 2011). This is consistent with the result from the kinematical information. The line list for the determination of chemical abundances is compiled from the Zhao et al. (2016), Jacobson & Friel (2013) and Neves et al. (2009).

The projected rotation velocity is helpful to distinguish the episodes from different sources, such as the internal and external origin. Following Carlberg et al. (2012), we derived the projected rotational velocity of TYC 3251-581-1 by fitting the unblended Fe I lines at 6750.2, 6733.2, and 6726.7 Å. We derived a low projected rotational velocity of 2.2 km s^{-1} using this method.

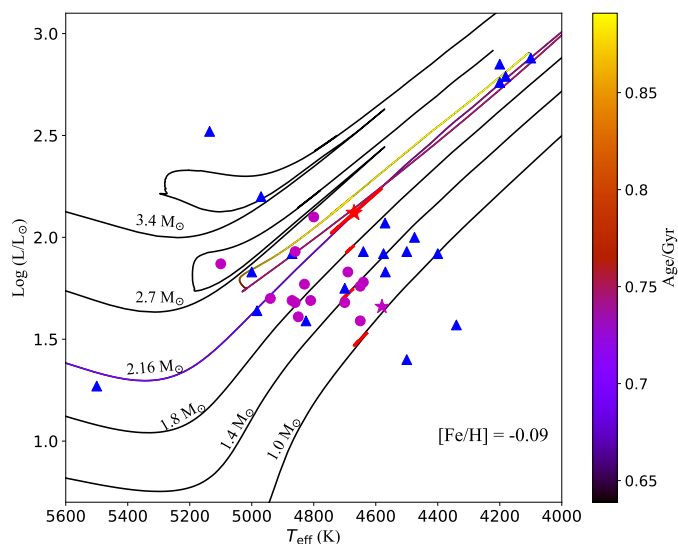


Fig. 3. TYC 3251-581-1 is indicated as a red star in the BaSTI tracks with metallicity $Z = 0.014$ (Pietrinferni et al. 2004), and the magenta star is the star HD 77361 (Kumar & Reddy 2009). The Charbonnel & Balachandran (2000) sample with $[\text{Fe}/\text{H}] = -0.46 \sim 0.10$ dex is denoted as the blue triangles, while the magenta points show the Kumar et al. (2011) sample with metallicities ranging from -0.27 to 0.18 dex. The location of the RGB bump is indicated by the red bold line at each track.

4. Discussion

According to the BaSTI tracks (Pietrinferni et al. 2004), TYC 3251-581-1 is close to the region of RGB bump in Hertzsprung-Russell diagram (see Fig. 3) with a mass $M = 2.16 M_{\odot}$ and age = 0.72 Gyr. Regarding the Li rich giants at the RGB bump, Charbonnel & Balachandran (2000) suggested that the enhanced Li caused by the extra mixing would again be decreased when the carbon isotopic ratio drops due to the deeper mixing processes. It implies that the enriched Li would take place prior the signature of reduction of $^{12}\text{C}/^{13}\text{C}$. This scenario may coincide with the Li-rich giants with high $^{12}\text{C}/^{13}\text{C}$ ($\geq \sim 20$), but it is not consistent with our derived super Li-rich giant with a low $^{12}\text{C}/^{13}\text{C}$ of ~ 9.0 . Recently Kumar et al. (2011) discovered a dozen Li-rich giant with low $^{12}\text{C}/^{13}\text{C}$, and the star HD 77361 is also located at the RGB bump.

One of the external mechanisms to increase the Li abundance of a star is to engulf a planet or a brown dwarf, as first suggested by Alexander (1967), which probably happens anywhere along the RGB. To reach the meteoritic Li abundance, an accreted planet of two Jupiter masses (M_{Jup}) should have an Li abundance of $A(\text{Li}) \sim 6$, based on the assumptions of Carlberg et al. (2010), this planet is so anomalous that Li abundance is much higher than the meteoritic abundance of the solar system. Moreover, Siess & Livio (1999) modelled the accretion of substellar companions (SSCs) by the solar-mass RGB star. They explored the possibly observational features for engulfing SSCs included IR emission, Li overabundance, and rotational velocity. All observed signatures are compatible with the accretion of SSCs, however the difficulty their scenario encountered is that the very high Li abundance requires a huge amount of Li accretion, so it can not properly account for the very high Li abundance (> 2.8 dex). Recently, Aguilera-Gómez et al. (2016b) considered the different typical masses and various metallicities of the giants for this episode, their calculations showed that the SSCs with mass higher than $15 M_{\text{Jup}}$ would be dissolved in the radiative zone rather than in the convective envelope. Thus, if there is no

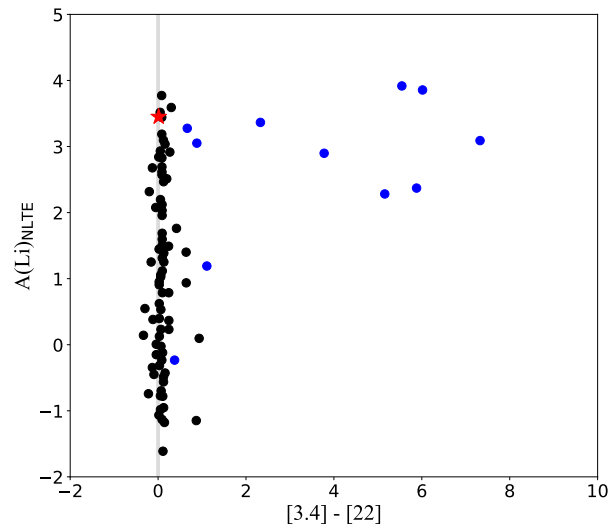


Fig. 4. $A(\text{Li})_{\text{NLTE}}$ vs. $[3.4]-[22]$ for the sample stars of Rebull et al. (2015). The vertical line at $[3.4]-[22]=0$ indicates the photospheric locus. The blue points denote sources identified with IR excess by Rebull et al. (2015), while the black ones are for these with no obvious IR excess. The red star is our target.

any extra mixing, the largest Li abundance could be achieved at 2.2 dex by engulfing the SSCs with a mass of $15 M_{\text{Jup}}$. In the case of external pollution, the external sources increase not only the Li materials, other light element abundances (^6Li , ^9Be and ^{11}B) and isotope ratio ($^{12}\text{C}/^{13}\text{C}$) (Siess & Livio 1999; Israelian et al. 2001) but also the orbital angular momentum. This scenario is unlikely for TYC 3251-581-1 due to it being super Li-rich, the low carbon isotopic ratio, and $v \sin i \sim 2.2 \text{ km s}^{-1}$.

It was suggested by de la Reza et al. (1997) that enhanced lithium is associated with IR excesses for K giants. In their model, the normal Li-poor K giants would turn out to be Li-rich caused by the internal mixing during a short period ($\sim 10^5 \text{ yr}$), which would result in an expansion of the circumstellar shell along with the mass loss (see also Drake et al. 2002; de la Reza et al. 2015). To check the scenario for our target, we extracted IR magnitudes of TYC 3251-581-1 at $[3.4, 4.6, 12$ and $22 \mu\text{m}$ bands] from WISE (Cutri & et al. 2013), following the procedure described by Rebull et al. (2015), and plot $A(\text{Li})_{\text{NLTE}}$ as a function of $[3.4]-[22]$ in Fig. 4. It shows our target with the 176 red giants from the cleanest possible sample of Rebull et al. (2015). Here $[3.4]-[22]$ is defined as the difference in magnitudes of these two bands. Rebull et al. (2015) also defined $\chi_{[3.4],[22]}$ as:

$$\chi_{[3.4],[22]} = \frac{([3.4]-[22])_{\text{observed}} - ([3.4]-[22])_{\text{predicted}}}{\sigma_{([3.4]-[22])}}$$

where $\sigma_{([3.4]-[22])}$ is quadratic sum of the errors on $3.4 \mu\text{m}$ and $22 \mu\text{m}$. $([3.4]-[22])_{\text{predicted}}$ is expected to be 0.0 for the K giant, which implies that the giant is without any circumstellar dust. $\chi_{[3.4]-[22]} \geq 3.0$ is set as the criterion for significant IR excess. The $\chi_{[3.4],[22]}$ for TYC 3251-581-1 is 0.36, much lower than the value of criterion, which clearly shows that TYC 3251-581-1 does not have IR excess at $[3.4]-[22]$. The result is consistent with that of Rebull et al. (2015), who shows in their Fig. 19 that the slow rotators are not likely to have IR excess. Furthermore, if Li-rich giants experienced mass-loss in the form of gas, their $H\alpha$ line profiles are likely asymmetrical or shifted (Reddy et al.

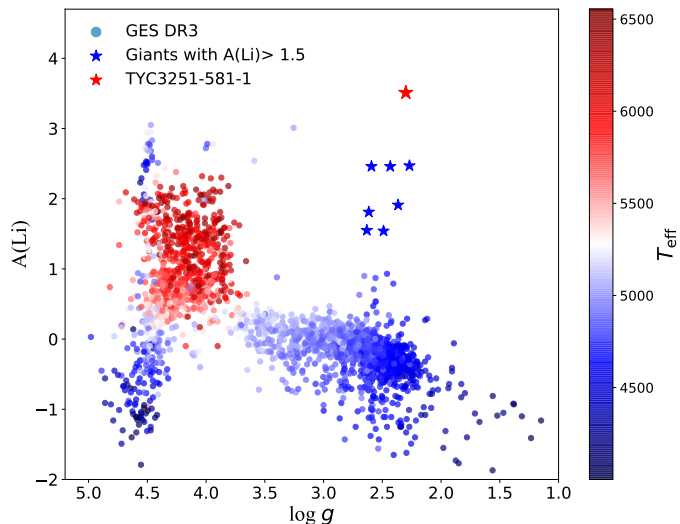


Fig. 5. $A(\text{Li})$ evolution plotted by $\log g$ in the Gaia-ESO DR3 with $[\text{Fe}/\text{H}] = -0.2 \sim 0.0$. The magenta star shows the TYC 3251-581-1, while the blue stars are the Li-rich giants discovered by Casey et al. (2016).

2002; Mészáros et al. 2009). There is no evidence for either asymmetry or a shift in the spectra of our target. In this case, the connection between infrared excess and the Li enhancement seems to be disfavoured by our data.

To intuitively inspect the Li abundance varying with the evolutionary stage, Fig. 5 (similar as the Fig. 3 of Aguilera-Gómez et al. 2016a) shows $A(\text{Li})$ versus $\log g$ for stars in the Gaia-ESO DR3³ with the metallicity ranged from -0.2 to 0.0. There are seven giants with Li abundance higher than the conventional criterion ($A(\text{Li}) \geq 1.5$ dex) of Li-rich. Three of them with $A(\text{Li}) > 2.0$ locate at the evolutionary stage before the RGB bump, they can be explained by the external scenario (Casey et al. 2016). Given similar metallicity, TYC 3251-581-1 pops up around the RGB bump with a much higher Li abundance than the maximum value of 2.2 dex predicted by Aguilera-Gómez et al. (2016b). In order to compare with the Li normal giant at the chemical view, we selected the star 17562024-4134502 from the Gaia-ESO DR3 which has similar atmospheric parameters to TYC 3251-581-1. A comparison of element-to-element abundances between the two stars is illustrated in Fig. 6. The detailed chemical abundances of star 17562024-4134502 from Li to Eu are presented in the Gaia-ESO DR3 catalogue. If the mass transfers from the evolved AGB companion to the star, the s-process elements (e.g. Ba) are expected to be enhanced together with the Li. The Ba abundance is approximately solar, and agrees with the prediction by Bisterzo et al. (2017) for the Galactic thin disc star. Thus, the external scenario of mass transfer seems to be inappropriate for our target. Except for Li, no evident differences on element abundances are found. It is consistent with the conclusion of other works (Martell & Shetrone 2013; Casey et al. 2016), that the abnormal high Li abundance is unlikely connected with other elemental abundances.

A large Li-rich sample was displayed in a plot of $A(\text{Li})$ versus $^{12}\text{C}/^{13}\text{C}$ by Rebull et al. 2015 (their Figure 21) and only three Li-rich giants are located at the region that has $A(\text{Li})$ exceeding the meteoritic value and $^{12}\text{C}/^{13}\text{C} \leq 15$. In the metallicity range of our target, only one star from Rebull et al. (HD 77361, also shown in Fig. 3) is also in the RGB bump re-

gion of the Hertzsprung-Russell diagram. TYC 3251-581-1 resembles HD 77361 in that it has high Li abundance and also low $^{12}\text{C}/^{13}\text{C}$ ratio, as well as similar atmospheric parameters (Lyubimkov et al. 2015). It does imply that the similar Li enrichment mechanisms might affect both of them. HD 77361 exhibits no IR excess (Rebull et al. 2015) with the low rotational velocity of 4.5 km s^{-1} (Lyubimkov et al. 2015), it seems to be in accordance with the suggestion that HD 77361 is likely to internally produce substantial Li (Kumar & Reddy 2009). HD 77361 also belongs to the thin disc population from the spatial velocities ($U_{\text{LSR}}, V_{\text{LSR}}, W_{\text{LSR}} = (46, 24, -5) \text{ km s}^{-1}$). From the point of Guiglion et al. (2016), the thin disc stars could be suffered higher Li enrichment than the thick disc stars due to the contribution of low mass stars. However, the contamination from the external sources is not expected to happen with respect to the low rotational velocity and non-IR excess. The decreased $[\text{C}/\text{Fe}]$ and enhanced $[\text{N}/\text{Fe}]$ of TYC 3251-581-1 imply that an extra mixing should have taken place before or at the bump, and the relatively low $^{12}\text{C}/^{13}\text{C}$ is in agreement with this suggestion. Interestingly, the $^{12}\text{C}/^{13}\text{C} \sim 9.0$ of TYC 3251-581-1 is lower than that of the prediction (19 ~ 23) of the extra mixing (e.g. thermohaline mixing Charbonnel & Lagarde 2010; $\delta\mu$ -mixing Eggleton et al. 2008) for Li-rich at the end of FDU. More observations, such as asteroseismology information, are required to provide more constraints to explain this anomaly.

5. Conclusions

In summary of our analysis, TYC 3251-581-1 lies close to the RGB bump evolution stage, as shown in Fig. 3, where extra-mixing can happen and induce Cameron-Fowler mechanism to enhance lithium. Our derived low carbon isotopic ratio, along with the low carbon abundance and enhanced nitrogen abundance suggest that the deep mixing have taken place in this star. However, for the super Li-rich giant with a low $^{12}\text{C}/^{13}\text{C}$ near the bump, the trigger of extra mixing is still ambiguous; further studies are needed to better understand the mechanisms of Li enhancement.

Acknowledgements. This research was supported by National Key Basic Research Programme of China 2014CB845700, and by the National Natural Science Foundation of China under grant Nos. 11603037 and 11473033. This work is supported by the Astronomical Big Data Joint Research Center, co-founded by the National Astronomical Observatories, Chinese Academy of Sciences and the Alibaba Cloud. K.P. acknowledges supports from the Mt. Cuba Astronomical Foundation Grant and from Center for Astronomical Mega-science, CAS. Guoshoujing Telescope (the Large Sky Area Multi-Object Fiber Spectroscopic Telescope LAMOST) is a National Major Scientific Project built by the Chinese Academy of Sciences. Funding for the project has been provided by the National Development and Reform Commission. LAMOST is operated and managed by the National Astronomical Observatories, Chinese Academy of Sciences. This publication makes use of data products from the Wide field Infrared Survey Explorer, which is a joint project of the University of California, Los Angeles, and the Jet Propulsion Laboratory/California Institute of Technology, funded by the National Aeronautics and Space Administration. Based on data products from observations made with ESO Telescopes at the La Silla Paranal Observatory under programme ID 188.B-3002.

References

- Adamów, M., Niedzielski, A., Villaver, E., et al. 2015, *A&A*, 581, A94
- Adamów, M., Niedzielski, A., Villaver, E., Wolszczan, A., & Nowak, G. 2014, *A&A*, 569, A55
- Adibekyan, V. Z., Santos, N. C., Sousa, S. G., & Israelian, G. 2011, *A&A*, 535, L11
- Adibekyan, V. Z., Sousa, S. G., Santos, N. C., et al. 2012, *A&A*, 545, A32
- Aguilera-Gómez, C., Chanamé, J., Pinsonneault, M. H., & Carlberg, J. K. 2016a, *ApJ*, 833, L24

³ <https://www.gaia-eso.eu>

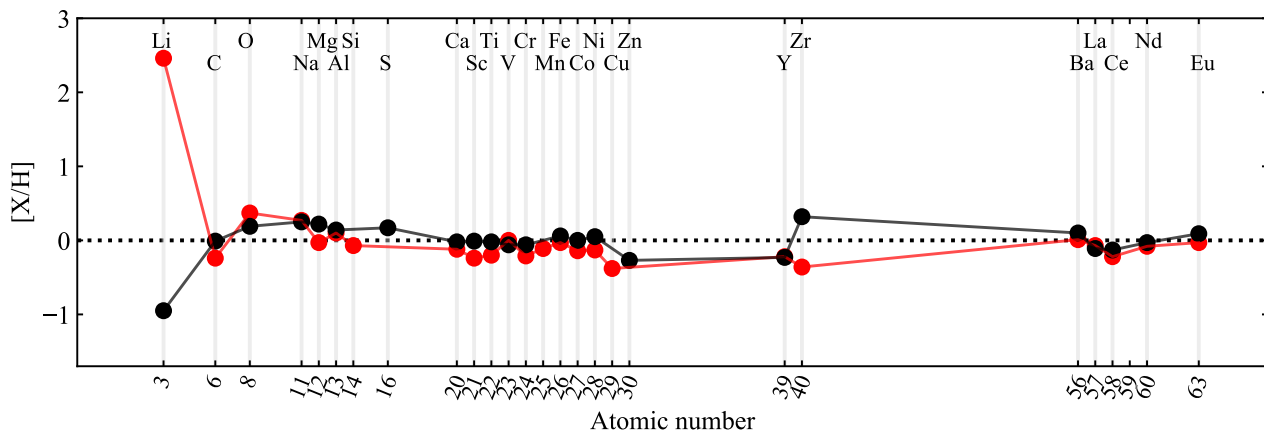


Fig. 6. Comparison of detailed chemical abundances between the super Li-rich giant TYC 3251-581-1 and the Li normal giant 17562024-4134502, which are shown in red and black respectively.

Table 2. Derived chemical abundances for TYC 3251-581-1

Species	Value $\pm \sigma^a$
A(Li) _{LTE} (6708 Å)	3.68 \pm 0.26
A(Li) _{NLTE} (6708 Å)	3.48 \pm 0.19
A(Li) _{LTE} (6104 Å)	3.38 \pm 0.13
A(Li) _{NLTE} (6104 Å)	3.53 \pm 0.13
¹² C/ ¹³ C	9.0 \pm 1.5
[C I/Fe]	-0.34 \pm 0.10
[N I/Fe]	0.33 \pm 0.01
[O I/Fe]	0.20
[Na I/Fe]	0.25 \pm 0.02
[Mg I/Fe]	0.06 \pm 0.04
[Al I/Fe]	0.13 \pm 0.02
[Si I/Fe]	0.03 \pm 0.06
[Ca I/Fe]	-0.08 \pm 0.03
[Sc II/Fe]	0.03 \pm 0.05
[Ti I/Fe]	-0.16 \pm 0.07
[Ti II/Fe]	-0.02 \pm 0.07
[V I/Fe]	0.18 \pm 0.05
[Cr I/Fe]	-0.09 \pm 0.03
[Mn I/Fe]	-0.10 \pm 0.04
[Co I/Fe]	0.02 \pm 0.01
[Ni I/Fe]	0.01 \pm 0.05
[Cu I/Fe]	-0.32 \pm 0.01
[Y II/Fe]	-0.10 \pm 0.03
[Zr I/Fe]	-0.15 \pm 0.05
[Ba II/Fe]	0.09 \pm 0.02
[La II/Fe]	0.08
[Ce I/Fe]	-0.01 \pm 0.01
[Nd II/Fe]	0.06 \pm 0.01
[Eu II/Fe]	0.10

Notes. ^(a) For Li, the σ denotes the quadratic sum of uncertainties due to the atmospheric parameters, and σ is the uncertainty of the spectral synthesis fit for ¹²C/¹³C and N, while it represents the standard deviation of the elemental abundances from the individual lines for the remaining elements.

Aguilera-Gómez, C., Chanamé, J., Pinsonneault, M. H., & Carlberg, J. K. 2016b, *ApJ*, 829, 127
 Alexander, J. B. 1967, *The Observatory*, 87, 238
 Alexeeva, S. A. & Mashonkina, L. I. 2015, *MNRAS*, 453, 1619
 Alonso, A., Arribas, S., & Martínez-Roger, C. 1999, *A&AS*, 140, 261
 Asplund, M., Grevesse, N., Sauval, A. J., & Scott, P. 2009, *ARA&A*, 47, 481
 Bisterzo, S., Travaglio, C., Wiescher, M., Käppeler, F., & Gallino, R. 2017, *ApJ*, 835, 97
 Brown, J. A., Sneden, C., Lambert, D. L., & Dutchover, Jr., E. 1989, *ApJS*, 71, 293
 Cameron, A. G. W. & Fowler, W. A. 1971, *ApJ*, 164, 111
 Carlberg, J. K., Cunha, K., Smith, V. V., & Majewski, S. R. 2012, *ApJ*, 757, 109
 Carlberg, J. K., Smith, V. V., Cunha, K., Majewski, S. R., & Rood, R. T. 2010, *ApJ*, 723, L103

Casey, A. R., Ruchti, G., Masseron, T., et al. 2016, *MNRAS*, 461, 3336
 Charbonnel, C. & Balachandran, S. C. 2000, *A&A*, 359, 563
 Charbonnel, C. & Lagarde, N. 2010, *A&A*, 522, A10
 Charbonnel, C. & Zahn, J.-P. 2007, *A&A*, 467, L15
 Cui, X.-Q., Zhao, Y.-H., Chu, Y.-Q., et al. 2012, *Research in Astronomy and Astrophysics*, 12, 1197
 Cutri, R. M. & et al. 2013, *VizieR Online Data Catalog*, 2328
 de la Reza, R., Drake, N. A., da Silva, L., Torres, C. A. O., & Martin, E. L. 1997, *ApJ*, 482, L77
 de la Reza, R., Drake, N. A., Oliveira, I., & Rengaswamy, S. 2015, *ApJ*, 806, 86
 Drake, N. A., de la Reza, R., da Silva, L., & Lambert, D. L. 2002, *AJ*, 123, 2703
 Eggleton, P. P., Dearborn, D. S. P., & Lattanzio, J. C. 2008, *ApJ*, 677, 581
 Gaia Collaboration, Brown, A. G. A., Vallenari, A., et al. 2016, *A&A*, 595, A2
 Grupp, F., Kurucz, R. L., & Tan, K. 2009, *A&A*, 503, 177
 Guiglion, G., de Laverny, P., Recio-Blanco, A., et al. 2016, *A&A*, 595, A18
 Hög, E., Fabricius, C., Makarov, V. V., et al. 2000, *A&A*, 355, L27
 Iben, Jr., I. 1967a, *ApJ*, 147, 650
 Iben, Jr., I. 1967b, *ApJ*, 147, 624
 Israelian, G., Santos, N. C., Mayor, M., & Rebolo, R. 2001, *Nature*, 411, 163
 Jacobson, H. R. & Friel, E. D. 2013, *AJ*, 145, 107
 Kirby, E. N., Guhathakurta, P., Zhang, A. J., et al. 2016, *ApJ*, 819, 135
 Kumar, Y. B. & Reddy, B. E. 2009, *ApJ*, 703, L46
 Kumar, Y. B., Reddy, B. E., & Lambert, D. L. 2011, *ApJ*, 730, L12
 Kupka, F., Piskunov, N., Ryabchikova, T. A., Stempels, H. C., & Weiss, W. W. 1999, *A&AS*, 138, 119
 Lebzelter, T., Utenthaler, S., Busso, M., Schultheis, M., & Aringer, B. 2012, *A&A*, 538, A36
 Li, H., Aoki, W., Matsuno, T., et al. 2018, *ApJ*, 852, L31
 Li, H., Aoki, W., Zhao, G., et al. 2016, in *IAU Symposium*, Vol. 317, *The General Assembly of Galaxy Halos: Structure, Origin and Evolution*, ed. A. Bragaglia, M. Arnaboldi, M. Rejkuba, & D. Romano, 51–56
 Lind, K., Asplund, M., & Barklem, P. S. 2009, *A&A*, 503, 541
 Lyubimkov, L. S., Kaminsky, B. M., Metlov, V. G., et al. 2015, *Astronomy Letters*, 41, 809
 Martell, S. L. & Shetrone, M. D. 2013, *MNRAS*, 430, 611
 Martin, E. L., Rebolo, R., Casares, J., & Charles, P. A. 1994, *ApJ*, 435, 791
 Mészáros, S., Dupree, A. K., & Szalai, T. 2009, *AJ*, 137, 4282
 Monaco, L., Boffin, H. M. J., Bonifacio, P., et al. 2014, *A&A*, 564, L6
 Monaco, L., Villanova, S., Moni Bidin, C., et al. 2011, *A&A*, 529, A90
 Neves, V., Santos, N. C., Sousa, S. G., Correia, A. C. M., & Israelian, G. 2009, *A&A*, 497, 563
 Palmerini, S., Cristallo, S., Busso, M., et al. 2011, *ApJ*, 741, 26
 Pfeiffer, M. J., Frank, C., Baumüller, D., Fuhrmann, K., & Gehren, T. 1998, *A&AS*, 130, 381
 Pietrinferni, A., Cassisi, S., Salaris, M., & Castelli, F. 2004, *ApJ*, 612, 168
 Rebull, L. M., Carlberg, J. K., Gibbs, J. C., et al. 2015, *AJ*, 150, 123
 Reddy, B. E., Lambert, D. L., & Allende Prieto, C. 2006, *MNRAS*, 367, 1329
 Reddy, B. E., Lambert, D. L., Hrivnak, B. J., & Bakker, E. J. 2002, *AJ*, 123, 1993
 Reetz, J. K. 1991, *Diploma Thesis*, Universität München
 Sackmann, I.-J. & Boothroyd, A. I. 1999, *ApJ*, 510, 217
 Shi, J. R., Gehren, T., Zhang, H. W., Zeng, J. L., & Zhao, G. 2007, *A&A*, 465, 587
 Siess, L. & Livio, M. 1999, *MNRAS*, 308, 1133
 Silva Aguirre, V., Ruchti, G. R., Hekker, S., et al. 2014, *ApJ*, 784, L16
 Wallerstein, G. & Sneden, C. 1982, *ApJ*, 255, 577
 Zhao, G., Mashonkina, L., Yan, H. L., et al. 2016, *ApJ*, 833, 225
 Zhao, G., Zhao, Y.-H., Chu, Y.-Q., Jing, Y.-P., & Deng, L.-C. 2012, *Research in Astronomy and Astrophysics*, 12, 723

Table 3. Changes in NLTE correction for the two Li lines

	Shi et al. (2007)	Lind et al. (2009)	ΔT_{eff} (80 K)	$\Delta \log g$ (0.2 dex)	$\Delta[\text{Fe}/\text{H}]$ (0.1 dex)	$\Delta \xi_{\text{t}} 0.2$ (km s^{-1})
$\Delta_{\text{NLTE}} 6708 \text{ \AA}$	-0.20	-0.22	-0.27	-0.33	-0.01	-0.01
$\Delta_{\text{NLTE}} 6104 \text{ \AA}$	0.15	0.18	0.14	0.13	0.14	0.13